Is 24(S)-hydroxycholesterol a potent modulator of cholesterol metabolism in Müller cells? An in vitro study about neuron to glia communication in the retina

Elise Léger Charnay, Elodie A.Y. Masson, Tristan Morala, Lucy Martine, Bénédicte Buteau, Laurent Leclere, Lionel Brétillon, Ségolène Gambert

HAL Id: hal-02622461
https://hal.inrae.fr/hal-02622461

Submitted on 21 Dec 2021

Is 24(S)-hydroxycholesterol a potent modulator of cholesterol metabolism in Müller cells? An in vitro study about neuron to glia communication in the retina

Elise LEGER-CHARNAY[1]; Elodie A.Y. MASSON[1]; Tristan MORALA[1]; Lucy MARTINE[1]; Bénédicte BUTEAU[1]; Laurent LECLERE[1]; Lionel BRETILLON[1]; Ségolène GAMBERT[1,2]

[1] Centre des Sciences du Goût et de l'Alimentation, AgroSup Dijon, CNRS, INRA, Université Bourgogne Franche-Comté, F-21000 Dijon, France.

[2] Laboratoire de Biochimie Médicale, Plateforme de Biologie Hospitalo-Universitaire, F-21000 Dijon, France

Corresponding author:
Ségolène GAMBERT
INRA-UMR CSGA
17, rue Sully
BP 86510
21065 DIJON
FRANCE
Phone: (+33)3.80.69.36.87; FAX: (+33)3.80.69.32.23; Email: segolene.gambert@chu-dijon.fr

Declarations of interest: none

ABBREVIATIONS: 24S-OHC: 24(S)-hydroxycholesterol; 27-OHC: 27-hydroxycholesterol; 27-COOH: 3β-hydroxy-5-cholestenoïc acid; 7KC: 7-ketocholesterol; 7β-OHC: 7β-hydroxycholesterol; ABCA1: ATP binding cassette subfamily A member 1; ApoE: Apolipoprotein E; CYP27A1: Cytochrome P450 family 27 subfamily A member 1; CYP46A1: Cytochrome P450 family 46 subfamily A member 1; DMEM: Dulbecco's modified Eagle's medium; EtOH: Ethanol; FBS: Foetal bovine serum; GC-FID: Gas chromatography coupled to flame ionization detector; GC-MS: Gas chromatography coupled to mass spectrometry; Gusb: β-glucuronidase; HMGCR: HMG-CoA reductase; LDL-R: Low density lipoprotein receptor; LXR: Liver X receptor; RQ: Relative quantification; SR-BI: Scavenger receptor class B member 1; SREBP: Sterol regulatory element-binding protein.

1. INTRODUCTION

The retina is a nervous tissue, comprising neurons and glial cells. The Müller cells are the major macroglial cells of the retina and support neuronal functioning. They cross the retina in a radial pattern, forming metabolic exchanges with neurons of all cell layers, providing nutrients, eliminating waste and more globally maintaining retinal homeostasis (Reichenbach and Bringmann, 2013). Among the homeostatic processes that are crucial for retinal health, one of them concerns a lipid found in every cell of higher animals: cholesterol.

Cholesterol is an amphiphilic lipid involved in many physiological processes. This is an important structural component of cell membranes, essential for modulating their fluidity, and thus signal transduction, membrane trafficking, ligand binding, etc. (Subczynski et al., 2017). Cholesterol can be entirely synthetized from acetyl-CoA through more than 30 consecutive reactions (Fig. 1), with HMG-CoA reductase (HMGCR) catalyzing the rate limiting and irreversible step of the process. From lanosterol, two pathways have been classically described: the Bloch pathway (Bloch et al., 1965) characterized by the precursor desmosterol, and the Kandutsch-Russell pathway characterized by another precursor, lathosterol (Kandutsch and Russell, 1960). The Bloch and Kandutsch-Russell pathways produce various intermediates that may have different bioactive effects on cells, including on cholesterol metabolism regulation, but also on other diverse cellular processes (Mitsche et al., 2015).

In the brain, cholesterol comes exclusively from *in situ* biosynthesis since the blood-brain barrier is not permeable to lipoproteins (Dietschy and Turley, 2004). Although all nucleated cells can synthesize cholesterol, some cell types do it more efficiently. Brain astrocytes have been proposed to produce cholesterol primarily by the Bloch pathway, supplying it to neighboring neurons (Nieweg et al., 2009; Pfrieger, 2003). Glial apolipoprotein E (ApoE) particles containing cholesterol are lipidated due to ATP-binding cassette A1 (ABCA1) transporter activity and can be captured by neurons or other cells via lipoprotein receptors, such as low-density lipoprotein receptor (LDL-R) and scavenger receptor B1 (SR-BI). Cerebral cholesterol efflux is mainly mediated by its conversion into 24(S)-hydroxycholesterol (24S-OHC), synthesized by the neuronal enzyme CYP46A1 (Russell et al., 2009). In the retina, cholesterol metabolism is less well characterized. Even though cholesterol-rich blood lipoproteins can cross the outer blood-retinal barrier, Lin et al. (2016) identified local synthesis as the main source of retinal cholesterol in the mouse. Müller cells have been shown to express HMGCR enzyme and secrete ApoE, suggesting their ability to synthesize and deliver cholesterol to neurons (Amaratunga et al., 1996; Fliesler and Bretillon, 2010). However, further evidence is needed to determine if Müller cells can, like astrocytes in the brain, act as cholesterol providers for retinal neurons. Retinal cholesterol elimination can be mediated by lipoprotein efflux, due to ABCA1 activity, or by oxysterol synthesis. 24S-OHC and 3β-hydroxy-5-cholestenoïc acid (27-COOH) are the major oxysterols found in the retina (Pikuleva and Curcio, 2014). Similarly to the brain, CYP46A1 expression in the retina is restricted to neurons, mainly to retinal ganglion cells (Bretillon et al., 2007), contrary to CYP27A1, the enzyme producing 27-COOH, which is more ubiquitous (Lee et al., 2006).

Nervous tissues are particularly dependent on cholesterol metabolism, notably because neurons have a high requirement for cholesterol since they permanently synthesize membranes for neurotransmitter exocytosis and dendritic spine growth. Nevertheless, cholesterol overload has been shown to be associated with neuronal death (Ayciriex et al., 2017), especially in the context of pathologies such as Alzheimer's disease and age-related macular degeneration (Pikuleva and Curcio, 2014; Puglielli et al., 2003). Hence, multiple feedback mechanisms exist in cells to sharply regulate key proteins related to cholesterol and maintain homeostasis. These mechanisms act at a transcriptional level, especially via liver X receptor (LXR) and sterol regulatory element-binding protein (SREBP) pathways, and at a post-translational level to modulate protein activity or degradation. Oxysterols, including 24S-OHC, have been shown to strongly activate some of the cholesterol regulatory pathways in various cells (Olkkonen et al., 2012). Considering the complementarity between neurons and glial cells in nervous tissues, constant neuron-glia crosstalk is

crucial for the maintenance of cholesterol homeostasis. As a cholesterol-derived product, specifically synthetized by neurons, 24S-OHC may represent a signaling molecule informing glial cells of the neuronal cholesterol content. It has been described that 24S-OHC stimulates ABCA1 and ApoE expression in brain astrocytes (Abildayeva et al., 2006; Liang et al., 2004). However, no published data demonstrate the effect of 24S-OHC on cholesterol metabolism in retinal Müller cells.

In the present study, using primary cultures of retinal Müller cells we provide some new insights on cholesterol metabolism and its regulation in the retina.

2. METHODS

2.1. Reagents

Dulbecco's modified Eagle's medium (DMEM) with phenol red, Trypsin-EDTA (0.05 % trypsin in PBS) and Penicillin-Streptomycin (10,000 U/m and 10 mg/ml respectively) were bought from PanBiotech (Dutscher, Brumath, France). Fetal bovine serum (FBS, lot 013BS986) was purchased from Biosera (Boussens, France). Collagenase was bought from Sigma-Aldrich (C2674, Sigma, St Quentin-Fallavier, France). 24S-OHC powder, purchased from Sigma-Aldrich (SML1648, Sigma, St Quentin-Fallavier, France), was solubilized in absolute ethanol (EtOH) (20 mM) and kept at -20 °C for long term storage. Diluted stock solutions (200 times more concentrated than treatment media) were prepared in EtOH and keep at -20 °C for up to one month. Treatment media at 0.5 µM or 1.5 µM 24S-OHC were freshly prepared in DMEM 1 g/L glucose + 10 % FBS, before each experiment. The control condition contained EtOH alone at the same concentration as treatment media (1:200, v/v). Standards and deuterated standards for quantification by mass-spectrometry were purchased from Aventi Polar Lipids (Interchim, Montluçon, France), except for Betulin bought from Sigma-Aldrich (St Quentin-Fallavier, France).

2.2. Animals

Long Evans rats, initially purchased form Charles River Laboratories (L'Arbresle, France), were maintained in our animal facility. Animals were housed in a controlled temperature (22±1 °C), 12h dark/light cycle and pathogen-free environment. Food and water were provided *ad libitum*. All experiments were conducted in accordance with the local ethic committee (University of Burgundy, Dijon, France) and the French ministry of Higher Education and Research.

2.3. Müller cell culture

Primary Müller cell cultures were generated as previously described by Hicks and Courtois (1990). Briefly, 8-12 days new-born rats were beheaded. Eyeballs were digested in a 2 % trypsin, 70 U/ml collagenase mix, for 50 minutes at 37 °C. Retinas were dissected and explants were cultured in DMEM 4.5 g/L glucose + 10 % FBS. When several cell islets were observed, explants were removed, medium replaced with DMEM 1g/L glucose + 10 % FBS, and cells allowed to reach confluence. Cultures were used after 2 passages. Cells were seeded in T150 flasks for sterol quantification or in T75 flasks for gene expression measurement. For the study of 24S-OHC effects, cells were incubated at about 80 % confluence with EtOH vehicle (control cells), 0.5 or 1.5 µM 24S-OHC for 48 hours. The purity of Müller cell cultures was assessed in 4 independent cultures by double immunofluorescence staining for glial fibrillary acidic protein (GFAP) a marker of astrocytes and Müller cells, and glutamine synthetase (GS), considered a specific marker of Müller cells. For this purpose, cells were seeded in µDish (Ibidi® 35mm high, 0.1×10^5 cells per dish) and fixed at sub-confluence with 4 % paraformaldehyde during 15 minutes. Blocking and permeabilization steps were performed for 1 hour at room temperature with a solution of PBS 1X, 1 % BSA, 0.1 % Triton X100, and 0.05 % Tween. Cells were then incubated with primary antibodies (mouse anti-GFAP, Interchim AYZ280, 1/100 and rabbit anti-GS, Abcam, G2781, 1/5000, diluted in blocking buffer) overnight at 4 °C, washed with

PBS 1X and incubated with secondary antibodies Alexa-Fluor 594 goat anti-mouse IgG and Alexa-fluor 488 goat anti-rabbit IgG (A11005, A11008, Life Technologies, 1/700) for 1 hour at room temperature. Cell nuclei were visualized with DAPI (4', 6-diamidino-2-phenylindole). Images of four representative fields per dish were acquired with a Leica Confocal microscope equipped with a 40X objective. They indicated that our cultures were exclusively Müller cells (Supplemental Fig.1).

2.4. Gene expression analysis by Taqman™ real time polymerase chain reaction

Cells were rinsed twice with PBS, collected by scraping and stored at -80°C until RNA isolation, which was performed using the Nucleospin® RNA/protein kit (Macherey-Nagel, Hoerdt, Farnce) according to manufacturer's instructions. Reverse transcription was operated using the Quantitec® Reverse Transcription Kit (Qiagen, Courtaboeuf, France) with 500 ng RNA per reaction. qPCR were prepared with 20 ng cDNA, TaqMan® Gene Expression Master Mix and TaqMan® probes (TaqMan® Gene Expression-Single tube assays, Thermofisher scientific, Life technologies, Courtaboeuf, France). For primer references, see Table 1. Plates were run on a StepOnePlus™ Real-Time PCR system (Applied biosystem, Thermofisher scientific) with cycle profile as denaturing at 95 °C for 20 s followed by 40 cycles at 95 °C for 1 s and 60 °C for 20 s. β-glucuronidase (Gusb) expression was used as a reference to normalize cDNA amounts. The expression level of this constitutively expressed control gene was not affected by our experimental conditions. Ct values were calculated by the StepOne v2.3 software from automatic threshold and baseline. The amplification efficiency of all TaqMan gene expression assays was considered to be 100 % according to manufacturer's data. ΔCt (Ct (gene of interest)-Ct (Gusb)) were used to compare the expression level of each gene of interest. To determine the effect of 24S-OHC exposure, relative quantification (RQ) values were calculated by the StepOne v2.3 using the $2^{-\Delta\Delta Ct}$ method. Three replicates, cultured in three independent T75 flasks, were used for each experimental condition in each primary Müller cell culture. These replicates were used to perform independent reverse transcriptions.

2.5. Sterol quantification by gas chromatography

Cells were rinsed twice with PBS, collected by scraping and stored at -80 °C until used. Samples, corresponding to 4 T150 flasks combined, were mechanically homogenized in water and homogenates were mixed with 5 volumes of chloroform-methanol (2:1, v:v) (Folch et al., 1957). Total lipids were collected in the lower chloroform phase and dried under a stream of nitrogen. For sterol and oxysterol quantification, except 27-COOH, assays were carried out following the procedure described in Fourgeux et al. (2012). In brief, total lipids were submitted to alkaline hydrolysis. Material that could not be saponified, containing sterols, was extracted in chloroform. Cholesterol was quantified from 1/10 of the total non-saponified material, after trimethylsilyl ether derivation and addition of 2 µg 5α-cholestane as a standard, by gas chromatography coupled to a flame ionization detector (GC-FID) (HP4890A, Hewlett-Packard, DB-5MS column, Agilent, Santa Clara, CA). In the remaining 9/10 of the non-saponified fraction, deuterated standards and betulin were added: 200 ng [26,26,26,27,27,27-^{2}H$_6$] desmosterol, 100 ng [25,26,26,26,27,27,27-^{2}H$_7$] lathosterol, 50 ng [25,26,26,26,27,27,27-^{2}H$_7$] 24S-OHC. Samples were purified on silica columns (Supelco®, Sigma, St Quentin-Fallavier, France) and derivatized to trimethylsilyl ethers. Cholesterol precursors and oxysterols were quantified by gas chromatography coupled to mass spectrometry (GC-MS) (5973N, Agilent; DB-5MS column, Agilent, Santa Clara, CA). Sterols were identified in SCAN mode according to their specific spectra and retention times defined by unlabelled standards. Sterols were quantified in SIM mode with the ions (m/z) listed in Table 2. For 27-COOH quantitation, 300 ng [25,25,26,26,26-^{2}H$_5$] 27-COOH were added to total lipids. Samples were not submitted to alkaline hydrolysis but directly purified on silica columns, according to the protocol mentioned above for cholesterol precursor and oxysterol quantitation. After diazomethane and trimethylsilyl ether derivations, 27-COOH was quantified using GC-MS (Table 2).

Absolute sterol amounts were determined by extrapolation from unlabelled standard curves. Quantities were then normalized to protein content. For this purpose, small aliquots of homogenized samples were submitted to Ripa 5X lysing buffer and proteins were quantified using the Pierce™ BCA assay (Fisherscientific, Illkirch, France).

2.6. Statistical analysis

Results were submitted to non-parametric statistical analysis. Wilcoxon matched-pairs signed rank tests were performed with GraphPad Prism6 software. All data are represented as mean ± S.D. and statistical significance is indicated as *p<0.05, **p<0.01.

3. RESULTS

3.1. Characterization of basal cholesterol metabolism in Müller cells

Quantitative measurements of sterols in primary Müller cultures were performed using GC-FID (cholesterol) and GC-MS (precursors and oxysterols). As shown in Table 3, we found that Müller cells contained typical cholesterol-related sterols including cholesterol precursors, cholesterol and oxysterols. With 45.8 ± 12.3 µg/mg of protein, cholesterol was clearly the most abundant sterol in cells. Except for lanosterol, which was detected at low amounts, cholesterol precursors of both the Bloch and Kandutsch-Russel pathways were found in significant quantities (zymosterol: 1.4 ± 0.6 µg/mg, desmosterol: 365.8 ± 80.4 ng/mg, and lathosterol: 287.8 ± 77.1 ng/mg). Regarding oxysterols, 24S-OHC was not detected in Müller cells. Similarly, neither 27-hydroxycholesterol (27-OHC) nor 27-COOH, the common CYP27A1 products, were found in Müller cells. On the contrary, non-enzymatic oxysterols, including 7-ketocholesterol (7KC) and 7 β-hydroxycholesterol (7β-OHC) were detected in significant amounts.

Using RT-qPCR we also analysed the expression of 10 genes involved in cholesterol metabolism, covering aspects of biosynthesis (HMGCR), uptake (LDL-R and SR-B1), export and elimination (ApoE, ABCA1 and CYP27A1) as well as regulation (SREBP2 and LXRα,β). Results presented in Figure 2 classified these genes according to their level of expression relative to a housekeeping gene (Gusb) used as an endogenous control. Every gene of interest exhibited a measurable expression in our Müller cell cultures, but LXRα and CYP46A1 expression were very low (ΔCt>4). This is in accordance with the literature, reporting that CYP46A1 exhibits a neuronal pattern (Bretillon et al., 2007) and that LXRα expression is very low in the retina (Zheng et al., 2015; Zheng et al., 2012). CYP27A1 gene expression appeared to be slightly higher (ΔCt=3.6) followed by ABCA1 (ΔCt=2.9). With a ΔCt lower than 1.5, LXRβ, SR-BI, HMGCR, SREBP2, ApoE and LDL-R genes were the most highly expressed among the tested targets in Müller cells.

Collectively, these data indicate that Müller cells possess the necessary cholesterol metabolism machinery suggesting that they could participate in cholesterol maintenance in the retina.

3.2. Effect of 24S-OHC on cholesterol metabolism in Müller cells

To determine the impact of 24S-OHC exposure on cholesterol metabolism in Müller cells, cultures were incubated with 0.5 µM or 1.5 µM 24S-OHC for 48 hours and used to perform sterol quantitation using GC-FID/MS (Fig. 3) or gene expression analysis using RT-qPCR (Fig. 4). The concentrations used for 24S-OHC treatments were not cytotoxic for Müller cells, as evaluated by cell viability assay (data not shown). First, we confirmed the efficacy of our treatment conditions to increase 24S-OHC levels in Müller cultures: undetected in untreated cells, it reached 333 ± 72 and 1338 ± 309 ng/mg protein, following 0.5 and 1.5 µM treatment, respectively (Fig. 3). Secondly, we measured a significant decrease in cholesterol levels in cells following 24S-OHC exposure at 1.5 µM (-37 % compared to control), while a smaller reduction was observed at 0.5µM (-15 %). These observations

demonstrate that 24S-OHC has a strong hypocholesterolemic effect on Müller cells in a dose-dependent manner.

We further investigated the mechanisms underlying this effect, especially endogenous cholesterol biosynthesis and cholesterol uptake/elimination pathways. We first looked at 2 major cholesterol precursors, typical of the different cholesterol biosynthetic pathways. As shown in Figure 3, the incubation of cells with 1.5 µM 24S-OHC led to a significant decrease in both desmosterol (-38 %) and lathosterol (-84 %). As evidenced by the considerable reduction in lathosterol levels, the Kandutch-Russel pathway is more impacted than the Bloch pathway by 24S-OHC. This is also supported by the fact that 24S-OHC at 0.5 µM was able to decrease lathosterol but not desmosterol levels. The decrease in cholesterol precursor levels was associated with a strong downregulation of HMGCR gene expression (2.4 fold decrease at 1.5 µM compared to control) (Fig. 4), confirming the inhibitory effect of 24S-OHC on cholesterol synthesis in Müller cells. Furthermore, in response to 1.5 µM 24S-OHC treatment *LDL-R* and *SR-BI* gene expression were reduced 2 fold and 1.6 fold respectively, suggesting decreased lipoprotein uptake by cells. This was concomitant with a dramatic increase in expression of *ABCA1* as well as increased *ApoE* gene expression (10 fold and 1.5 fold increase at 1.5 µM, respectively), supporting enhanced cholesterol efflux via ApoE-rich lipoproteins. 24S-OHC induced a small but significant overexpression of *CYP27A1*, also supporting an increase in cholesterol elimination. We also analyzed the expression of *LXRβ* and *SREBP* genes, transcription factors which were found to be significantly expressed in our in vitro Müller glia model. While *LXRβ* expression was not altered by 24S-OHC exposure, *SREBP2* was down-regulated in 1.5 µM 24S-OHC-treated cells (1.5 fold decrease), suggesting the possible involvement of this transcription factor in the observed modulation of cholesterol metabolism. Exposure to the lower dose of 24S-OHC (0.5 µM) showed similar tendencies to to 1.5 µM but exhibited statistical significance only for decreased *HMGCR,* and increased *ABCA1,* gene expression. These results suggest that these two genes, and particularly *ABCA1*, are more responsive to transcriptional regulation by 24S-OHC.

Altogether these data indicate that 24S-OHC is a potent signalling molecule in Müller cells, decreasing cholesterol levels via both down-regulation in cholesterol biosynthesis and uptake, and upregulation in cellular cholesterol efflux.

4. DISCUSSION

While it has been shown clearly that the neural retina is able to synthesize cholesterol (Fliesler et al., 1993; Zheng et al., 2015), it is still unclear which cells are responsible for this production. As proposed by Pfrieger for astrocytes in the brain (Nieweg et al., 2009; Pfrieger, 2003), it is plausible that retinal glial cells could be providers of cholesterol for neurons. However literature data concerning expression of HMGCR, the rate-limiting enzyme of cholesterol biosynthetic pathway, in the principal glial population of the retina (Müller cells) are scarce. One study reports expression of this enzyme in rat retinal Müller cells, as well as rod inner segments and RPE, using immunohistochemistry and *in situ* hybridization (Fliesler and Bretillon, 2010). Two others showed HMGCR expression throughout the mouse and human retina, with the exception of the photoreceptor outer segments (Zheng et al., 2015; Zheng et al., 2012). We report here in Müller cell cultures the expression of *HMGCR* gene and high amounts of cholesterol, associated with the presence of several cholesterol precursors (lanosterol, zymosterol, desmosterol, and lathosterol), supporting the idea that these cells have the capacity to efficiently synthesize cholesterol. From the precursor lanosterol, cholesterol biosynthesis is known to occur through the Bloch and Kandutsch-Russell pathways, two enzymatic routes respectively characterized by desmosterol and lathosterol compounds. In our cultures, desmosterol and lathosterol were found in similar amounts, suggesting that Müller cells use the two pathways equally, contrary to brain astrocytes which mainly use the Bloch pathway (Nieweg et al., 2009). Furthermore, we detected robust gene expression of *ApoE* and its partner *ABCA1* transporter, suggesting that Müller cells are able to export the cholesterol they synthesize by releasing

nascent HDL-like particles, analogous to astrocytes in the brain (Ito et al., 2014). This is consistent with the idea developed by Tserentsoodol et al. (2006a) that HDL-like particles mediate intra-retinal cholesterol trafficking. These cholesterol-rich particles can be subsequently captured by surrounding neurons, which express LDL-R family receptors according to their cholesterol need.

Our Müller cell cultures also showed high expression of *LDL-R* and *SR-BI* genes, suggesting their ability to uptake or to remodel exogenous lipoprotein particles. LDL-R has already been localized in the retina by immunohistochemistry, especially within the retinal ganglion cell layer, which includes Müller cell processes, as well as in the outer plexiform layer, the retinal pigment epithelium and the choriocapillaries. In the same study, it was shown that the retina is able to take up blood-borne LDL (Tserentsoodol et al., 2006b). Our observations support the fact that Müller cells play a role in this process. SR-BI is a membrane receptor binding many lipoproteins, including high density lipoproteins (HDL), very low-density lipoproteins (VLDL) and LDL (Shen et al., 2014). Contrary to LDLR family receptors, SR-BI mediates bi- directional transport of cholesterol, depending on the cell type and demand. In liver and steroidogenic tissues, it enables cholesterol transport from lipoproteins to cells (Landschulz et al., 1996). On the contrary, in macrophages SR-BI enhances cellular cholesterol efflux to HDL (Ji et al., 1997). In nervous tissues, the role of SR-BI is still unclear. In the retina, it has been shown to be principally expressed by Müller cells (Tserentsoodol et al., 2005), consistent with the significant expression of SR-BI we observed in our cultures.

Altogether, these results support the idea developed by Fliesler and Bretillon (2010) that "Müller cells may participate in remodeling the lipid core of lipoproteins and delivery of lipids and nutrients to retinal neurons".

Exposure of Müller cultures to 24S-OHC led to increased intracellular amounts of this oxysterol proportional to the concentration of 24S-OHC added to the culture medium. This indicates that, in our model, 24S-OHC is readily incorporated by the cells. Due to their additional hydroxy group, side-chain oxysterols have a higher capacity to pass phospholipid bilayers than cholesterol (Bjorkhem, 2006; Meaney et al., 2002). A specific mechanism for oxysterol translocation through biological membranes, termed "bobbing", has recently been proposed by Kulig et al. (2018). In the retina, free 24S-OHC released by neurons into the extracellular matrix, could therefore readily diffuse into neighboring cells, especially Müller cells which ensheathe the neurons. Moreover, it is known that oxysterols are transported in lipoproteins in the systemic circulation, mainly as HDL in a free and esterified form (Burkard et al., 2007). As suggested by others and the current results, Müller cells express the molecular machinery, notably *ABCA1* and *ApoE* genes, to secrete discoid apoE and HDL-like particles, which thus surround retinal neurons. 24S-OHC could be included in these particles, thus being available for capture by cells, especially Müller cells, which express lipoprotein receptors.

Interestingly, we show that Müller cells can adjust their cholesterol metabolism in response to 24S-OHC. This oxysterol is an elimination product of cholesterol produced by neurons. It is also considered as a signaling molecule used by brain neurons to inform astrocytes of cholesterol status which in turn downregulate cholesterol synthesis. In line with this, our results show that Müller cells strongly downregulate cholesterol synthesis after 24S-OHC exposure. We found a higher reduction in lathosterol than desmosterol, indicating that the Kandutsch-Russell pathway is more sensitive to cholesterol metabolism regulation. This contrasts with a study on Chinese hamster ovary cells in which the Kandutsch-Russell pathway was shown to be constitutively active whereas the Bloch pathway was flexible in response to cholesterol availability and demand (Mitsche et al., 2015), indicating cellular specificities in cholesterol biosynthetic pathways.

In addition, our results indicate that Müller cells exposed to 24S-OHC decrease cholesterol uptake via LDL-R, and increase cholesterol efflux via ApoE-containing lipoproteins. Especially, the ABCA1 transporter is dramatically upregulated in response to 24S-OHC. This is in agreement with data showing that 24S-OHC induces ApoE-mediated efflux of cholesterol in a human astrocytoma cell line (Abildayeva et al., 2006). Since the blood-retina barrier, contrary to the blood-brain barrier, is permeable to lipoproteins this cholesterol efflux via ApoE-rich lipoproteins could be a pathway to

eliminate cholesterol from the retina and avoid toxic overload. By contrast, oxysterol synthesis does not appear to be a major route for cholesterol elimination in Müller cells. Compared to *ApoE* or *ABCA1*, gene expression of *CYP27A1*, the principal cholesterol hydroxylase in the retina, was only slightly increased. And despite this increase, we were unable to detect either of its products, 27-OHC and 27-COOH. This could be due to the fact that CYP27A1 protein levels and/or activity remain too low to translate into detectable products because of post-transcriptional and post-translational regulation, which have been described in the retina (Pikuleva and Curcio, 2014). Moreover, a study performed on monkey retina using immunohistochemistry detected CYP27A1 protein predominantly in the inner segment of photoreceptors, while Müller cells were only faintly stained (Lee et al., 2006). Nevertheless, one cannot exclude the possibility that 27-COOH synthetized by Müller cells is further converted into other unidentified oxysterol compound as has been described in neuroblastoma cells (Meaney et al., 2007). The absence of 24S-OHC, synthetized by CYP46A1, the other cholesterol hydroxylase found in the retina, is consistent with the very low gene expression we measured in our cells, and with the strictly neuronal origin of this compound (Bretillon et al. 2007; Ramirez et al. 2008). *SR-BI* gene expression was reduced in response to 24S-OHC. As we mentioned above, this receptor mediates bi- directional transport of cholesterol depending on cell type. Since 24S-OHC exposure activates hypocholesterolemic pathways in our Müller cells, this implies that SR-BI has a role in cholesterol-rich lipoprotein uptake rather than lipoprotein efflux in these cells.

As 24S-OHC-induced regulation occurred at the transcriptional level in our model, it suggests that 24S-OHC is able to modulate gene expression, most likely through interaction with nuclear receptors and transcription factors as has been described previously (Mutemberezi et al., 2016). We did not observe any upregulation of *LXR* gene expression in response to 24S-OHC, but this does not preclude upregulation of transcriptional activity, as has been shown in published data. However, we did see decreased SREBP2 transcript levels, a transcription factor which exerts hypercholesterolemic effects. This decrease could therefore contribute to the downregulation of cholesterol biosynthesis we observe in response to 24S-OHC exposure, since HMGCR is one of its targets (Burg and Espenshade, 2011). Typically, regulation of SREBP by oxysterols implicates two mediators, INSIG and SCAP, and is achieved through the prevention of its translocation to the Golgi and consecutive activation in the nucleus (Mutemberezi et al., 2016). Interestingly, in our model, it seems that 24S-OHC is able to regulate SREBP2 at the gene expression level.

Overall, the effects of 24S-OHC we observed suggest that Müller cells could participate in cholesterol homeostatic feedback in the retina, previously proposed by Pfrieger with astrocytes and neurons in the brain (Pfrieger and Ungerer, 2011). It corroborates the observations previously made using various *in vitro* models, that oxysterols are able to strongly regulate cholesterol (Abildayeva et al., 2006; An et al., 2017; Fu et al., 2001; Waltl et al., 2013). From these observations the idea arose that oxysterols are central players in cholesterol homeostasis maintenance. However, their importance *in vivo* remains under debate and studies conducted on animal models are not as concordant. For instance, Rosen et al. (1998) observed normal blood plasma levels of cholesterol in mice lacking the CYP27A1 enzyme, suggesting that 27-OHC is not necessary to maintain cholesterol homeostasis in the body. On the other hand, a study conducted by Chen et al. (2007) reported that the induction of LXR-target genes by a cholesterol-enriched diet was impaired by the deletion of 3 CYP enzymes related to oxysterol synthesis, in a transgenic mouse model. In a comprehensive review, Gill et al. (2008) proposed a revised hypothesis about the role of oxysterols in the regulation of cholesterol metabolism. They suggested that "while cholesterol is central to achieving its own balance, oxysterols play an important role in smoothing this regulation in the short term".

5. CONCLUSIONS

We show that Müller cells express the necessary machinery to synthesize and regulate cholesterol as well as lipoprotein remodeling, suggesting that they could play the role of cholesterol providers in the retina. We also demonstrate the capacity of Müller cells to activate a range of pathways lowering cholesterol levels in response to neuronal 24S-OHC (Fig. 5), supporting the idea that they actively participate in the maintenance of retinal cholesterol homeostasis via neuron-glia crosstalk. A better understanding of perturbations in this communication could offer new insights into the pathogenesis of neurodegenerative diseases.

Table. 1. References of TaqMan assays (Applied Bioscience) used for RT-qPCR analysis

Genes	Coding for	TaqMan assay references	Amplicon lenght
Hmgcr	HMGCR	Rn00565598_m1	71
Ldlr	LDL-R	Rn00598442_m1	76
Scarb1	SR-BI	Rn00580588_m1	75
Apoe	ApoE	Rn00593680_m1	99
Abca1	ABCA1	Rn00710172_m1	76
Cyp46a1	CYP46A1	Rn01430188_m1	72
Cyp27a1	CYP27A1	Rn01401086_m1	94
Nr1h3	LXRα	Rn00581185_m1	90
Nr1h2	LXRβ	Rn00581178_m1	75
Srebf2	SREBP2	Rn01502638_m1	61

Hmgcr: 3-hydroxy-3-methylglutaryl-CoA reductase, Ldlr: low density lipoprotein receptor, Scarb1: scavenger receptor class B member 1, Apoe: apolipoprotein E, Abca1: ATP binding cassette subfamily A member 1, Cyp46a1: cytochrome P450 family 46 subfamily A member 1, Cyp27a1: cytochrome P450 family 27 subfamily A member 1, Nr1h3 :nuclear receptor subfamily 1 group H member 3, Nr1h2: nuclear receptor subfamily 1 group H member 2, Srebf2: Sterol regulatory element-binding transcription factor 2.

Table. 2. Internal standards and ions for sterol quantification using mass-spectrometry in SIM mode.

			Internal standards				
			Desmosterol (d6)	Lathosterol (d7)	24S-OHC (d7)	27-COOH (d5)	Betulin
		m/z	333	465	152	417	496
	Lanosterol	393		x			
	Desmosterol	327	x				
	Zymosterol	456		x			
	Lathosterol	458		x			
Target molecules	24S-OHC	145			x		
	27-OHC	456					x
	27-COOH	412				x	
	7KC	472					x
	7β-OHC	456					x

Table 3. Sterol composition of Müller cell cultures.

	Sterols	Quantity / mg protein ± SD
	Cholesterol	45.8 µg ± 12.3
Cholesterol precursors	Lanosterol	1.1 ng ± 0.4
	Zymosterol	1.4 µg ± 0.6
	Desmosterol	365.8 ng ± 80.4
	Lathosterol	287.8 ng ± 77.1
Oxysterols	24S-OHC	nd
	27-OHC	nd
	27-COOH	nd
	7KC	274.9 ng ± 127
	7β-OHC	49.8 ng ± 2.3

Cells were cultured from new-born rat retinas. After two passages, they were collected at confluence and sterols were quantified by GC-FID (Cholesterol) or GC-MS (precursors and oxysterols). Cholesterol was found as the most abundant sterol in Müller cells. Cholesterol precursors typical of the Bloch and Kandutsch-Russell pathways, including desmosterol and lathosterol, were quantified at relatively high levels. Non-enzymatic oxysterols, 7KC and 7β-OHC were also detected. Sterol quantities were normalized to protein content. Data are indicated as mean ± S.D. of 3 independent cultures. nd: not detected.

DISCLOSURES

Declarations of interest: none

Figure Legends

Fig.1. Schematic representation of cholesterol biosynthesis and cholesterol oxidation pathways.
Cellular cholesterol synthesis is a complex process, beginning with acetyl-CoA. HMG-CoA reductase (HMGCR) catalyzing HMG-CoA conversion into mevalonate, is the rate limiting enzyme of the synthesis. From lanosterol, cholesterol can be synthetized by two distinct enzymatic routes, the Bloch and the Kandutsch-Russell pathways, comprising distinct cholesterol precursors.
Oxysterols are oxidation products of cholesterol. They arise from cholesterol by auto-oxidation (7-ketocholesterol (7KC) and 7β-hydroxycholesterol (7β-OHC) are typical cholesterol auto-oxidation products), or by enzymatic oxidation, usually involving the cytochrome P450 (CYP) family. CYP46A1 and CYP27A1 synthetize, 24(S)-hydroxycholesterol (24S-OHC) and 3β-hydroxy-5-cholestenoic acid (27-COOH), which are the major oxysterols found in the retina. CYP11A1, producing pregnenolone (Preg), is also expressed in the retina. More than being elimination products of cholesterol, oxysterols are also implicated in cholesterol metabolism regulation in various tissues.

Fig. 2. Müller cells express cholesterol metabolism machinery.
RT-qPCR was performed on Müller cell total cDNA. Gusb was chosen as the reference gene and ΔCt (Ct(gene of interest)-Ct(Gusb)) were calculated for each gene. The higher the ΔCt is, the lower the expression of the gene of interest. Every cholesterol-related gene was found to be expressed. The highest expression levels were measured for *LDL-R, ApoE, SREBP2, HMGCR, SR-BI* and *LXRβ*. *ABCA1* and *CYP27A1* gene expression occurred at lower levels. *LXRα* and *CYP46A1* transcripts were detected but their ΔCt values suggest very low expression in Müller cells.
Each bar represents the mean ± S.D. of 8 cultures. For each culture, triplicates were submitted to independent reverse transcription.

Fig.3. 24S-OHC has a strong hypocholesterolemic effect in Müller cells.
Cultures were incubated with EtOH vehicle (control) or 24S-OHC at 0.5 µM or 1.5 µM for 48 hours.
Sterols were quantified in cell pellets by GC-FID (cholesterol) or GC-MS (precursors and 24S-OHC).
Cholesterol and its precursors, desmosterol and lathosterol, were significantly reduced following 24S-OHC treatment at 1.5 µM. n=7 cultures in each group. Data are represented as mean ± S.D. * p<0.05 vs 24S-OHC at 0 µM (control) (Wilcoxon matched-pairs signed rank test). nd: not detected.

Fig.4. 24S-OHC activates a range of cholesterol lowering pathways in Müller cells.
Cultures were incubated with EtOH vehicle (control) or 24S-OHC at 0.5 µM or 1.5 µM for 48 hours.
Gene expression of cholesterol-related genes was assessed by RT-qPCR and data were analyzed using the $2^{-\Delta\Delta CT}$ method. Genes involved in cholesterol synthesis and cholesterol uptake were downregulated in cells treated with 24S-OHC at 1.5 µM. On the contrary, genes involved in cholesterol efflux were upregulated following 24S-OHC exposure. Each bar represents the mean ± S.D. of 8 cultures. For each culture, triplicates were submitted to independent reverse transcription. * p<0.05, **p<0.01 vs control (Wilcoxon matched-pairs signed rank test).

Fig. 5. Schematic representation of 24S-OHC effects on Müller cell cholesterol metabolism.
We showed that 24S-OHC at 1.5 µM leads to strongly decreased cholesterol content in Müller cells.
This occurs through decreased cholesterol synthesis, via *HMGCR* gene downregulation and reduction of cholesterol precursor amounts, an increase in cholesterol efflux, suggested by *ABCA1*, *ApoE* and *CYP27A1* gene upregulation, and a decrease in lipoprotein uptake via down-regulation of *LDL-R* and *SR-BI* gene expression. *SREBP2* gene expression is also downregulated suggesting that this transcription factor could participate in the above regulations. *CYP27A1* gene was found to be expressed, and was upregulated following 24S-OHC exposure, but the typical products of the enzyme (27-OHC, 27-COOH) were not detected.
Chol: cholesterol, Lano: lanosterol, Desmo: desmosterol, Latho: lathosterol.

Supplemental. Fig.1. High purity of Müller cultures.
Cells were double labelled with glial fibrillary acidic protein (GFAP, red), a general marker of macroglial cells, and glutamine synthetase (GS, green), a specific marker of Müller cells. Nuclei were stained with Dapi (blue). Results clearly showed that every cell positive for GFAP was also positive for GS. Moreover, we could find no cell (visible with DAPI staining) which was not positive for GS.
These observations indicate that our primary Müller cell cultures, after two passages and under our culture conditions, were indeed exclusively Müller cells. Negative control: no primary antibody. Scale bar: 50 µm.

REFERENCES

Abildayeva, K., Jansen, P.J., Hirsch-Reinshagen, V., Bloks, V.W., Bakker, A.H., Ramaekers, F.C., de Vente, J., Groen, A.K., Wellington, C.L., Kuipers, F., Mulder, M., 2006. 24(S)-hydroxycholesterol participates in a liver X receptor-controlled pathway in astrocytes that regulates apolipoprotein E-mediated cholesterol efflux. J Biol Chem 281, 12799-12808.

Amaratunga, A., Abraham, C.R., Edwards, R.B., Sandell, J.H., Schreiber, B.M., Fine, R.E., 1996. Apolipoprotein E is synthesized in the retina by Muller glial cells, secreted into the vitreous, and rapidly transported into the optic nerve by retinal ganglion cells. J Biol Chem 271, 5628-5632.

An, Y., Zhang, D.D., Yu, H.L., Ma, W.W., Lu, Y.H., Liu, Q.R., Xiao, R., 2017. 27-Hydroxycholesterol regulates cholesterol synthesis and transport in C6 glioma cells. Neurotoxicology 59, 88-97.

Ayciriex, S., Djelti, F., Alves, S., Regazzetti, A., Gaudin, M., Varin, J., Langui, D., Bieche, I., Hudry, E., Dargere, D., Aubourg, P., Auzeil, N., Laprevote, O., Cartier, N., 2017. Neuronal Cholesterol Accumulation Induced by Cyp46a1 Down-Regulation in Mouse Hippocampus Disrupts Brain Lipid Homeostasis. Front Mol Neurosci 10, 211.

Bjorkhem, I., 2006. Crossing the barrier: oxysterols as cholesterol transporters and metabolic modulators in the brain. Journal of internal medicine 260, 493-508.

Bloch, K., 1965. The biological synthesis of cholesterol. Science 150, 19-28.

Bretillon, L., Diczfalusy, U., Bjorkhem, I., Maire, M.A., Martine, L., Joffre, C., Acar, N., Bron, A., Creuzot-Garcher, C., 2007. Cholesterol-24S-hydroxylase (CYP46A1) is specifically expressed in neurons of the neural retina. Curr Eye Res 32, 361-366.

Burg, J.S., Espenshade, P.J., 2011. Regulation of HMG-CoA reductase in mammals and yeast. Prog Lipid Res 50, 403-410.

Burkard, I., von Eckardstein, A., Waeber, G., Vollenweider, P., Rentsch, K.M., 2007. Lipoprotein distribution and biological variation of 24S- and 27-hydroxycholesterol in healthy volunteers. Atherosclerosis 194, 71-78.

Chen, W., Chen, G., Head, D.L., Mangelsdorf, D.J., Russell, D.W., 2007. Enzymatic reduction of oxysterols impairs LXR signaling in cultured cells and the livers of mice. Cell metabolism 5, 73-79.

Dietschy, J.M., Turley, S.D., 2004. Thematic review series: brain Lipids. Cholesterol metabolism in the central nervous system during early development and in the mature animal. J Lipid Res 45, 1375-1397.

Fliesler, S.J., Bretillon, L., 2010. The ins and outs of cholesterol in the vertebrate retina. J Lipid Res 51, 3399-3413.

Fliesler, S.J., Florman, R., Rapp, L.M., Pittler, S.J., Keller, R.K., 1993. In vivo biosynthesis of cholesterol in the rat retina. FEBS Lett 335, 234-238.

Folch, J., Lees, M., Sloane Stanley, G.H., 1957. A simple method for the isolation and purification of total lipides from animal tissues. J Biol Chem 226, 497-509.

Fourgeux, C., Martine, L., Pasquis, B., Maire, M.A., Acar, N., Creuzot-Garcher, C., Bron, A., Bretillon, L., 2012. Steady-state levels of retinal 24S-hydroxycholesterol are maintained by glial cells intervention after elevation of intraocular pressure in the rat. Acta Ophthalmol 90, e560-567

Fu, X., Menke, J.G., Chen, Y., Zhou, G., MacNaul, K.L., Wright, S.D., Sparrow, C.P., Lund, E.G., 2001. 27-hydroxycholesterol is an endogenous ligand for liver X receptor in cholesterol-loaded cells. The Journal of biological chemistry 276, 38378-38387.

Gill, S., Chow, R., Brown, A.J., 2008. Sterol regulators of cholesterol homeostasis and beyond: the oxysterol hypothesis revisited and revised. Progress in lipid research 47, 391-404.

Hicks, D., Courtois, Y., 1990. The growth and behaviour of rat retinal Muller cells in vitro. 1. An improved method for isolation and culture. Exp Eye Res 51, 119-129.

Ito, J.I., Nagayasu, Y., Miura, Y., Yokoyama, S., Michikawa, M., 2014. Astrocytes endogenous apoE generates HDL-like lipoproteins using previously synthesized cholesterol through interaction with ABCA1. Brain Res 1570, 1-12.

Ji, Y., Jian, B., Wang, N., Sun, Y., Moya, M.L., Phillips, M.C., Rothblat, G.H., Swaney, J.B., Tall, A.R., 1997. Scavenger receptor BI promotes high density lipoprotein-mediated cellular cholesterol efflux. J Biol Chem 272, 20982-20985.

Kandutsch, A.A., Russell, A.E., 1960. Preputial gland tumor sterols. 3. A metabolic pathway from lanosterol to cholesterol. J Biol Chem 235, 2256-2261.

Kulig, W., Mikkolainen, H., Olzynska, A., Jurkiewicz, P., Cwiklik, L., Hof, M., Vattulainen, I., Jungwirth, P., Rog, T., 2018. Bobbing of Oxysterols: Molecular Mechanism for Translocation of Tail-Oxidized Sterols through Biological Membranes. The journal of physical chemistry letters 9, 1118-1123.

Landschulz, K.T., Pathak, R.K., Rigotti, A., Krieger, M., Hobbs, H.H., 1996. Regulation of scavenger receptor, class B, type I, a high density lipoprotein receptor, in liver and steroidogenic tissues of the rat. J Clin Invest 98, 984-995.

Lee, J.W., Fuda, H., Javitt, N.B., Strott, C.A., Rodriguez, I.R., 2006. Expression and localization of sterol 27-hydroxylase (CYP27A1) in monkey retina. Exp Eye Res 83, 465-469.

Liang, Y., Lin, S., Beyer, T.P., Zhang, Y., Wu, X., Bales, K.R., DeMattos, R.B., May, P.C., Li, S.D., Jiang, X.C., Eacho, P.I., Cao, G., Paul, S.M., 2004. A liver X receptor and retinoid X receptor heterodimer mediates apolipoprotein E expression, secretion and cholesterol homeostasis in astrocytes. J Neurochem 88, 623-634.

Lin, J.B., Mast, N., Bederman, I.R., Li, Y., Brunengraber, H., Bjorkhem, I., Pikuleva, I.A., 2016. Cholesterol in mouse retina originates primarily from in situ de novo biosynthesis. J Lipid Res 57, 258-264.

Meaney, S., Bodin, K., Diczfalusy, U., Bjorkhem, I., 2002. On the rate of translocation in vitro and kinetics in vivo of the major oxysterols in human circulation: critical importance of the position of the oxygen function. Journal of lipid research 43, 2130-2135.

Meaney, S., Heverin, M., Panzenboeck, U., Ekstrom, L., Axelsson, M., Andersson, U., Diczfalusy, U., Pikuleva, I., Wahren, J., Sattler, W., Bjorkhem, I., 2007. Novel route for elimination of brain oxysterols across the blood-brain barrier: conversion into 7alpha-hydroxy-3-oxo-4-cholestenoic acid. J Lipid Res 48, 944-951.

Mitsche, M.A., McDonald, J.G., Hobbs, H.H., Cohen, J.C., 2015. Flux analysis of cholesterol biosynthesis in vivo reveals multiple tissue and cell-type specific pathways. Elife 4, e07999.

Mutemberezi, V., Guillemot-Legris, O., Muccioli, G.G., 2016. Oxysterols: From cholesterol metabolites to key mediators. Prog Lipid Res 64, 152-169.

Nieweg, K., Schaller, H., Pfrieger, F.W., 2009. Marked differences in cholesterol synthesis between neurons and glial cells from postnatal rats. J Neurochem 109, 125-134.

Olkkonen, V.M., Beaslas, O., Nissila, E., 2012. Oxysterols and their cellular effectors. Biomolecules 2, 76-103.

Pfrieger, F.W., 2003. Outsourcing in the brain: do neurons depend on cholesterol delivery by astrocytes? Bioessays 25, 72-78.

Pfrieger, F.W., Ungerer, N., 2011. Cholesterol metabolism in neurons and astrocytes. Prog Lipid Res 50, 357-371.

Pikuleva, I.A., Curcio, C.A., 2014. Cholesterol in the retina: the best is yet to come. Prog Retin Eye Res 41, 64-89.

Puglielli, L., Tanzi, R.E., Kovacs, D.M., 2003. Alzheimer's disease: the cholesterol connection. Nat Neurosci 6, 345-351.

Ramirez, D.M., Andersson, S., Russell, D.W., 2008. Neuronal expression and subcellular localization of cholesterol 24-hydroxylase in the mouse brain. J Comp Neurol 507, 1676-1693.

Reichenbach, A., Bringmann, A., 2013. New functions of Muller cells. Glia 61, 651-678.

Rosen, H., Reshef, A., Maeda, N., Lippoldt, A., Shpizen, S., Triger, L., Eggertsen, G., Bjorkhem, I., Leitersdorf, E., 1998. Markedly reduced bile acid synthesis but maintained levels of cholesterol and vitamin D metabolites in mice with disrupted sterol 27-hydroxylase gene. The Journal of biological chemistry 273, 14805-14812.

Russell, D.W., Halford, R.W., Ramirez, D.M., Shah, R., Kotti, T., 2009. Cholesterol 24-hydroxylase: an enzyme of cholesterol turnover in the brain. Annu Rev Biochem 78, 1017-1040.

Shen, W.J., Hu, J., Hu, Z., Kraemer, F.B., Azhar, S., 2014. Scavenger receptor class B type I (SR-BI): a versatile receptor with multiple functions and actions. Metabolism 63, 875-886.

Subczynski, W.K., Pasenkiewicz-Gierula, M., Widomska, J., Mainali, L., Raguz, M., 2017. High Cholesterol/Low Cholesterol: Effects in Biological Membranes: A Review. Cell Biochem Biophys 75, 369-385.

Tserentsoodol, N., Gordiyenko, N.V., Pascual, I., Lee, J.W., Fliesler, S.J., Rodriguez, I.R., 2006a. Intraretinal lipid transport is dependent on high density lipoprotein-like particles and class B scavenger receptors. Mol Vis 12, 1319-1333.

Tserentsoodol, N., Sztein, J., Campos, M., Gordiyenko, N. V., Fariss, R. N., Lee, J. W., Fliesler, S. J., Rodriguez, I. R., 2006b. Uptake of cholesterol by the retina occurs primarily via a low density lipoprotein receptor-mediated process. Mol Vis 12, 1306-1318

Tserentsoodol, N., Gordiyenko, N.V., Lee, J.W., Rodriguez, I.R., 2005. Localization of scavenger receptors class B (SRBI.1 and SRBI.2) responsible for lipid transport in the retina. Invest. Ophthalmol Vis Sci 46:2992. ARVO annual meeting abstract.

Waltl, S., Patankar, J.V., Fauler, G., Nusshold, C., Ullen, A., Eibinger, G., Wintersperger, A., Kratky, D., Malle, E., Sattler, W., 2013. 25-Hydroxycholesterol regulates cholesterol homeostasis in the murine CATH.a neuronal cell line. Neuroscience letters 539, 16-21.

Zheng, W., Mast, N., Saadane, A., Pikuleva, I.A., 2015. Pathways of cholesterol homeostasis in mouse retina responsive to dietary and pharmacologic treatments. J Lipid Res 56, 81-97.

Zheng, W., Reem, R.E., Omarova, S., Huang, S., DiPatre, P.L., Charvet, C.D., Curcio, C.A., Pikuleva, I.A., 2012. Spatial distribution of the pathways of cholesterol homeostasis in human retina. PLoS One 7, e37926.

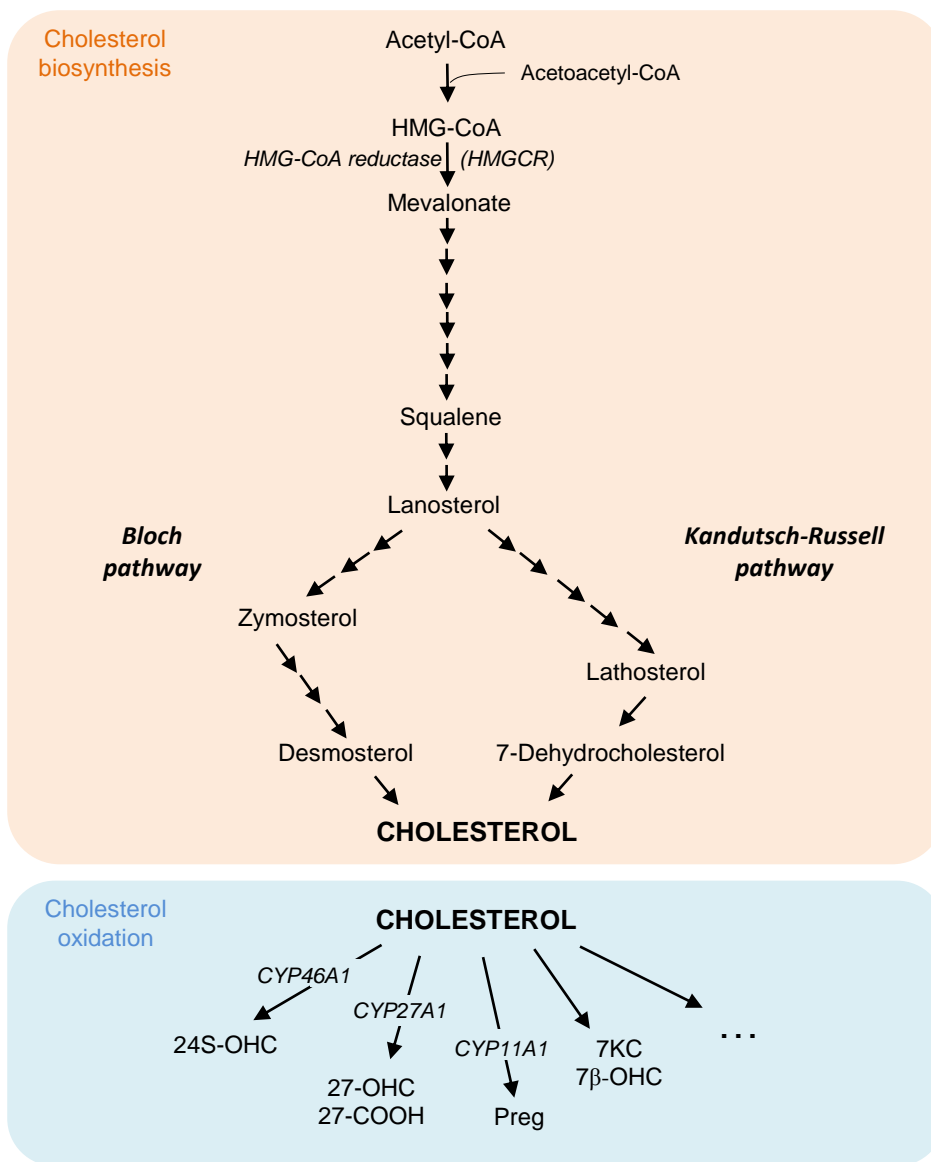**Fig.1.** Schematic representation of cholesterol biosynthesis and cholesterol oxidation pathways.

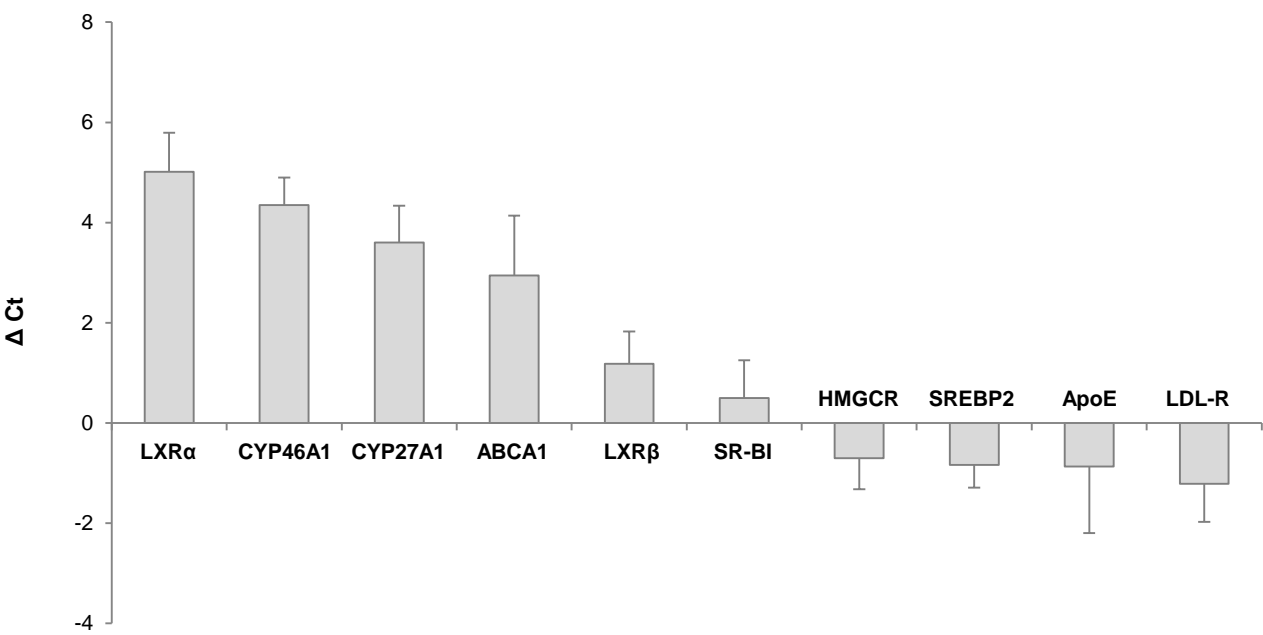**Fig. 2.** Müller cells express the cholesterol metabolism machinery.

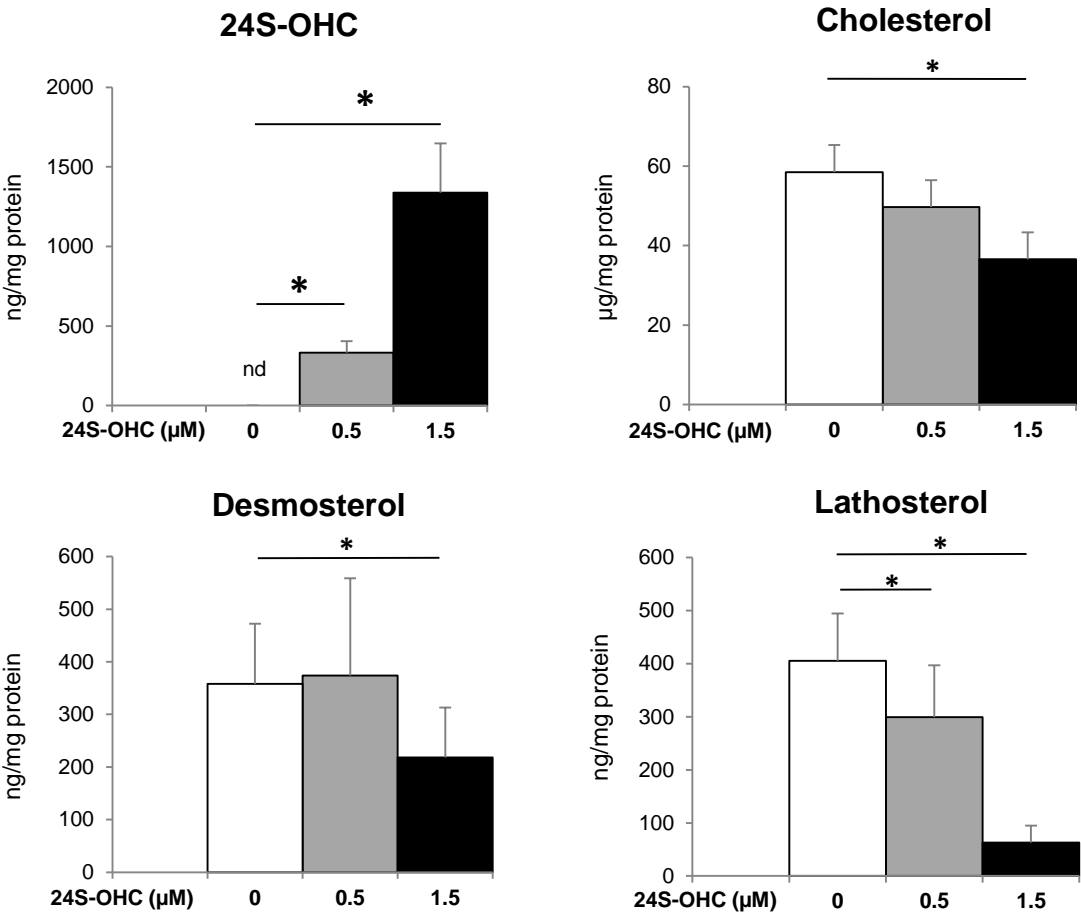**Fig.3.** 24S-OHC has a strong hypocholesterolemic effect in Müller cells.

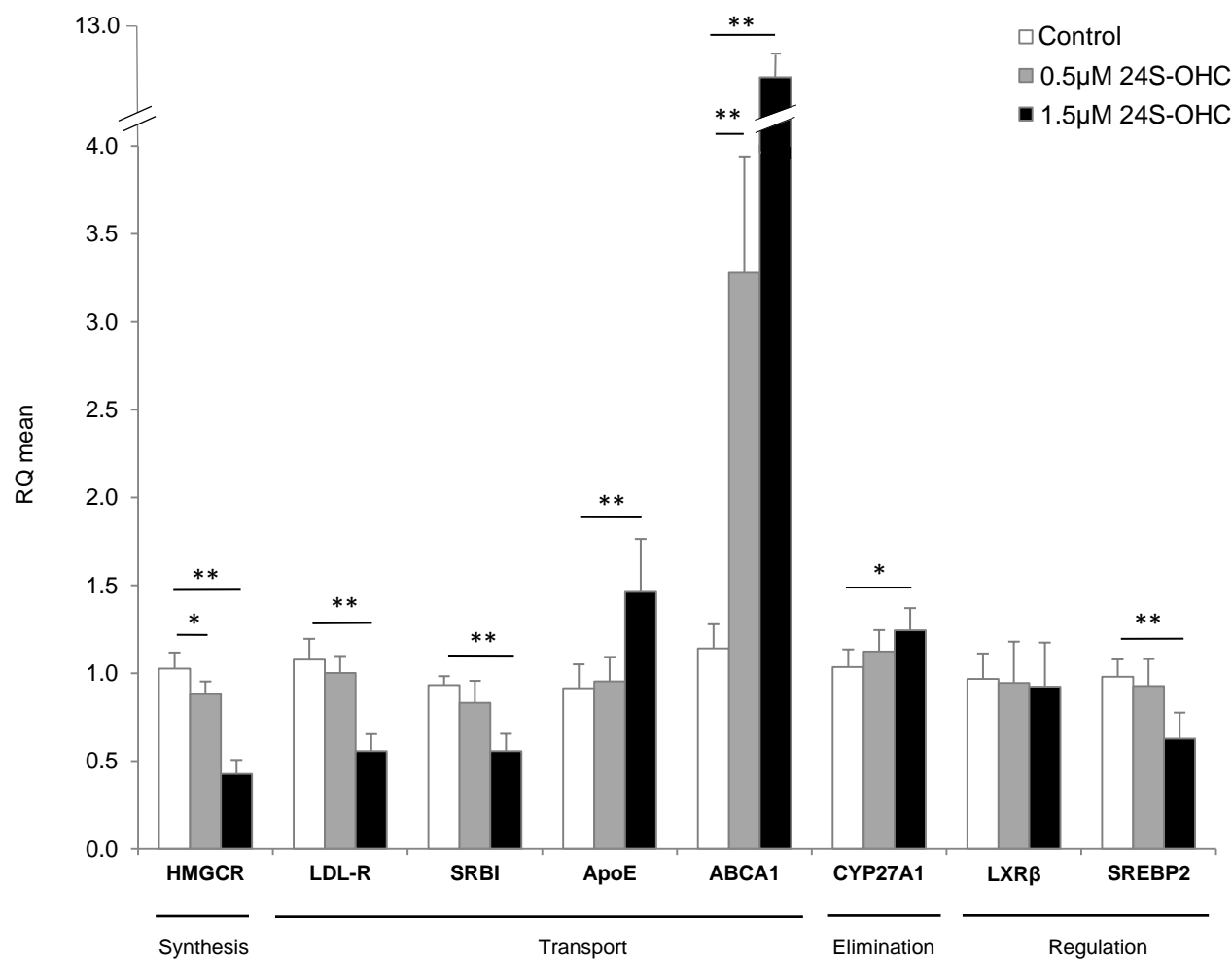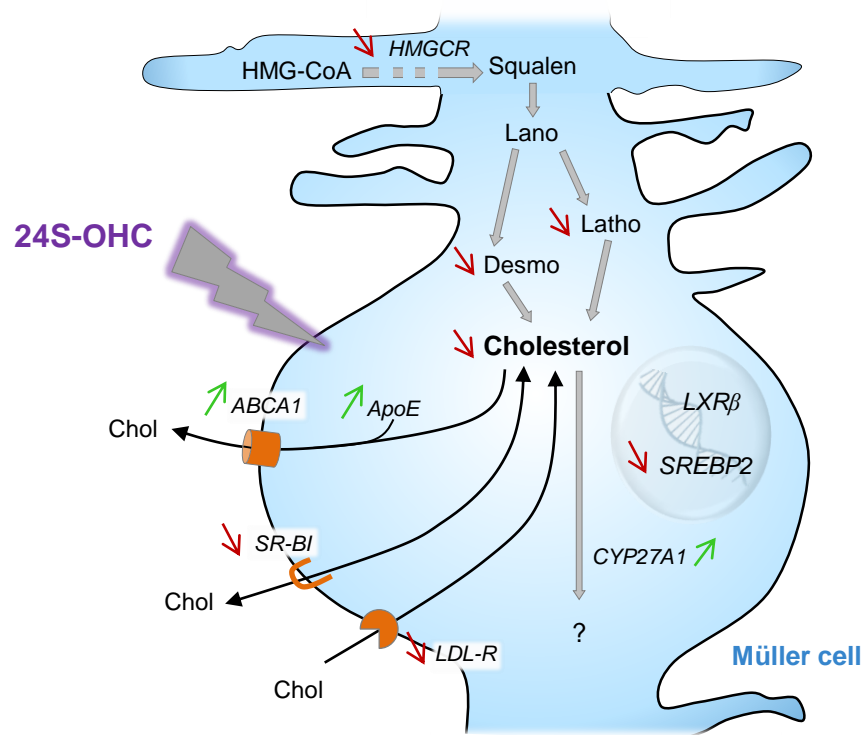**Fig.4.** 24S-OHC activates a range of cholesterol lowering pathways in Müller cells.

Fig. 5. Schematic representation of 24S-OHC effect on Müller cell cholesterol metabolism.

HIGHLIGHTS:

- Müller cells contain cholesterol-related sterols and express associated genes
- 24(S)-hydroxycholesterol (24S-OHC) depletes cholesterol levels in Müller cells
- 24S-OHC activates hypocholesterolemic mechanisms in Müller cells
- 24S-OHC downregulates genes involved in cholesterol synthesis and uptake
- 24S-OHC upregulates genes implicated in cholesterol efflux